APPLIED RESEARCH

Reduction of Crosstalk in the Electromyogram: Experimental Validation of the Optimal Spatio-Temporal Filter

MATTEO RAGGI [1], **GENNARO BOCCIA** [2], **AND LUCA MESIN** [1]

[1]Mathematical Biology and Physiology Research Group, Department of Electronics and Telecommunications, Politecnico di Torino, 10129 Turin, Italy
[2]NeuroMuscularFunction Research Group, Department of Clinical and Biological Sciences, University of Torino, 10126 Turin, Italy

Corresponding author: Luca Mesin (luca.mesin@polito.it)

ABSTRACT Objective: Crosstalk in surface electromyogram (EMG) is an important open problem and the common strategy of reducing it through spatial filters needs improvements. Methods: We evaluated experimentally the optimal spatio-temporal filter (OSTF), i.e., a recent approach that adapts to the subject, filtering different EMG channels both in time and space to emphasize the signal of a target muscle discarding that of adjacent ones. EMGs were recorded by a high-density recording system from pronator teres (target muscle) and flexor carpi radialis (crosstalk muscle) of 8 healthy subjects. OSTF was tested in different conditions, considering one channel per muscle (either single or double differential, SD and DD, respectively), changing the selectivity of detection (small electrodes close to each other, or large ones with higher inter-electrode distance), the force applied by the muscles (whose EMGs were summed to simulate different levels of crosstalk), and the duration of the signal to train the method. Results: OSTF was less affected by crosstalk than SD and DD filters. Statistically significant improvements were obtained in reducing the crosstalk-induced variations: for example, considering small electrodes, we obtained a percentage error of 157.30±57.11 % and 38.54±10.47 % (mean±std) in the estimation of the average rectified value (ARV), and an error of 23.57±3.92 % and 8.31±0.88 % in the estimation of the median frequency (MDF), for SD and OSTF, respectively. Conclusion: The OSTF can be applied in real-time, is easy to use, and is feasible even when using only few detection channels, as is customary in many applications.

INDEX TERMS Crosstalk, spatial filter, surface EMG.

I. INTRODUCTION

The surface electromyogram (EMG) is the electrical signal generated by a muscle during its contraction and recorded by electrodes placed over the skin [1]. These electrodes have a large pick-up volume [2], [3], so they record a mixture of contributions from the target muscle (i.e., the one to be investigated) and nearby muscles [4], [5], [6]. The latter is known as crosstalk [7]. Nowadays, crosstalk is still an open problem in surface EMG: indeed, it may affect the estimation

The associate editor coordinating the review of this manuscript and approving it for publication was Paolo Crippa [ID].

of muscle activity in different application studies, such as gait analysis [8], control of myoelectric prosthesis [9], [10], [11] and ergonomics for task evaluation [12].

Many authors investigated the effect of crosstalk, both in simulation [13], [14], [15], [16], [17] and experimentally [18], [19], [20], [21], [22], to better understand its biophysical origin and to provide a quantification of it. More specifically, some results showed that a quantification through cross-correlation of the signals of target and crosstalk muscles is not effective [23]. Furthermore, a temporal filter was found to be not useful to reduce this undesired contribution [6], [24].

The easiest strategy to avoid this issue is through an appropriate electrode positioning [25] in combination with spatial filters [18], [20]. Indeed, far-field potentials have an important common mode when recorded by different electrodes, in contrast to propagating components [26], [27]: thus, spatial filters removing efficiently common potentials can attenuate crosstalk. However, there are some limitations: type and dimension of electrodes used, physical properties of the tissue and anatomy of the subject affect the contribution of crosstalk, as demonstrated in simulated conditions [13], [14], [15], [16], [17]. Moreover, when selective spatial filters are used, only a small detection volume is analyzed, discarding also most of the EMG from the target muscle. This could be a problem if the recorded activity of the motor units (MU) included in this small detection volume is not representative of the whole muscle [28].

In literature, advanced strategies have also been introduced to quantify and remove the EMG of crosstalk muscles: for example, blind source separation (BSS) techniques [21], inverse methods [27], [29] and decomposition algorithms [30], [31]. However, these methods require high-density recording systems that are not common in applications and advanced processing, which probably limited their diffusion.

An alternative approach to both simple fixed spatial filters and complicated methods mentioned above was proposed in [32]: it is called optimal spatio-temporal filter (OSTF). Being a filter, it can be easily applied and used in real-time. Moreover, it requires simple recording systems (e.g., few EMG channels over target and crosstalk muscles). Only a preliminary complication is needed, i.e., the recording of selective signals from the target and the crosstalk muscles, on the basis of which the filter is optimized before being ready for application. Indeed, the OSTF should be adapted to the specific conditions (i.e., detection system and volume conductor anatomy, geometry and conductivity) in order to emphasize the energy of the target EMG and discard the one produced by crosstalk muscles. The method, which shares some features with the common spatial pattern (CSP [33]), is stable and was validated in simulation and with preliminary experimental data [32]. Moreover, it provided better performances than BSS techniques in a recent validation on surface EMG from finger extensor muscles [34]. In this work, we provide a deep experimental validation of the OSTF, considering EMG from pronator teres (PT, target muscle) and flexor carpi radialis (FCR, crosstalk muscle).

In the following sections, the theory of the method and its experimental validation are presented.

II. METHODS
A. DESIGN OF THE OPTIMAL FILTER
Filter coefficients are chosen by training on selective contractions of the target and crosstalk muscles. From now on, EMG relative to target muscles will be named as 'signal' $S_i(t)$, whereas the rest as 'crosstalk' $C_i(t)$. The index $i = 1, 2 \ldots, M$ indicates the ith EMG channel, while t the time samples. According to [35], an optimal spatial filter (OSF,

in the context of a brain-computer interface, BCI) can be obtained by combining a set of weights w_i that maximizes the signal to crosstalk ratio (SCR)

$$SCR = 10\log_{10} \frac{\left\| \sum_{i=1}^{M} w_i S_i(t) \right\|_2^2}{\left\| \sum_{i=1}^{M} w_i C_i(t) \right\|_2^2} \qquad (1)$$

where the sum of the weights $\{w_i\}_{i=1,\cdots,M}$ is equal to zero (in order to remove the common mode). Notice that an arbitrary scaling of the weights is possible without changing the SCR.

An analytical solution to the problem of maximizing the SNR is obtained as follows. First, if monopolar signals are used, the common mode should be removed by subtracting the mean over channels. Notice that this is not required if single differential (SD) or double differential (DD) signals are chosen as input channels, as the common mode has already been removed. Since the logarithm function in (1) is monotonically increasing, it is sufficient to maximize its argument. More in detail, the problem can be rewritten as the maximization of the following functional

$$J(w) = \frac{\left\| \sum_{i=1}^{M} w_i S_i(t) \right\|_2^2}{\left\| \sum_{i=1}^{M} w_i C_i(t) \right\|_2^2} = \frac{w^T R_S w}{w^T R_C w} \qquad (2)$$

where $w = \{w_i\}$ is the vector of weights, and R_S and R_C are signal and crosstalk autocorrelation matrices, respectively. Considering the arbitrary modulus of the vector of weights (mentioned above), we can fix to 1 the norm of the filter weights and write a constrained optimization problem, that can be solved by studying the Lagrangian

$$L_P = \frac{1}{2} w^T R_S w + \frac{1}{2} \lambda (1 - w^T R_C w) \qquad (3)$$

where λ is the Lagrange multiplier. Imposing the gradient with respect to the weights to be zero, the following relation is obtained [36]

$$R_S w = \lambda R_C w \rightarrow R_C^{-1} R_S w = \lambda w \qquad (4)$$

The change of variable $v = R_S^{1/2} w$ is then introduced, obtaining the following problem

$$R_S^{1/2} R_C^{-1} R_S^{1/2} v = \lambda v \qquad (5)$$

The matrix $R_S^{1/2} R_C^{-1} R_S^{1/2}$ is symmetric and positive definite so that it can be diagonalized, the eigenvalues are positive real numbers and the eigenvectors $\{v_k\}$ are orthogonal. Coming back to the problem for the filter weights, we can consider the following vectors corresponding to the eigenvectors $\{v_k\}$: $w_k = R_S^{-1/2} v_k$. The functional evaluation of such vectors is

$$J(w_k) = \frac{w_k^T R_S w_k}{w_k^T R_C w_k} = \lambda_k \qquad (6)$$
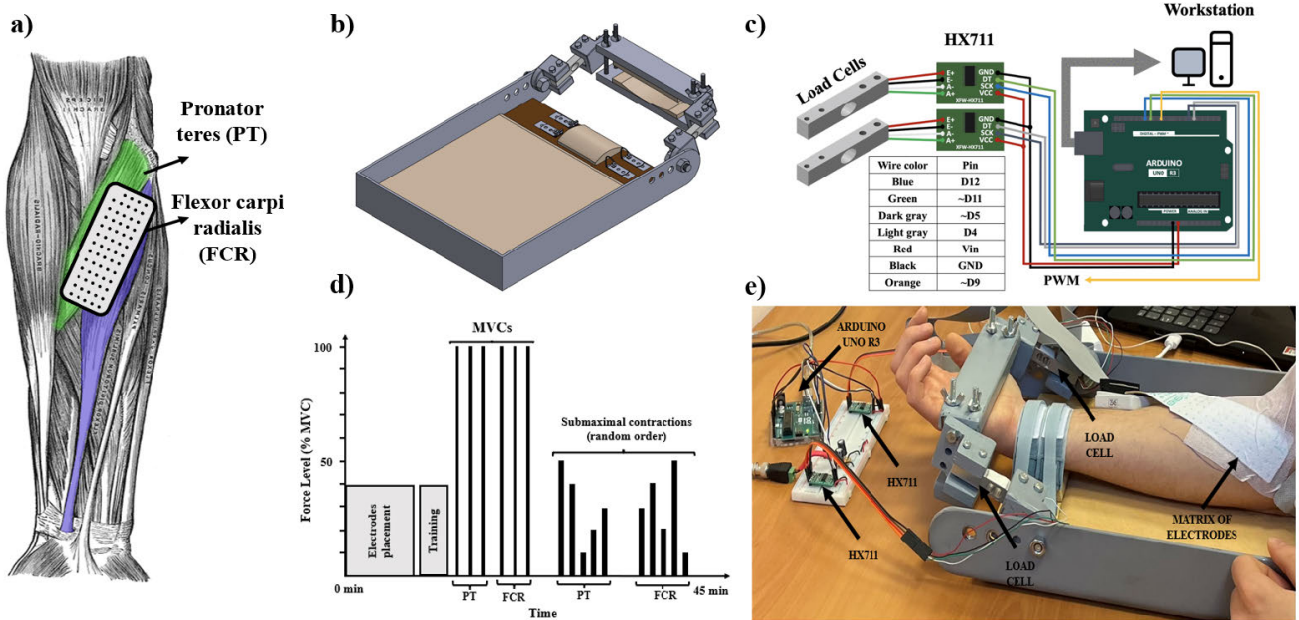
FIGURE 1. (a) Front view of the right forearm, with an indication of the investigated muscles: pronator teres (PT) and flexor carpi radialis (FCR). The matrix of electrodes used for this experimental protocol is placed so that two columns of electrodes are distributed on each muscle. The inter-electrode distance (IED) is equal to 8 mm. (b) Three-dimensional representation of the instrumentation used for the experimental protocol. (c) Electrical connections between load cells included in (b), the two ADC converters HX711 and the Arduino® UNO board (connected to the workstation via USB port). (d) Graphical resume of the experimental protocol. (e) Shot of the acquisition phase.

because $w_k^T R_S w_k = 1$ and $w_k^T R_C w_k = 1/\lambda_k$. In conclusion, the weights that maximize the SCR defined in (1) are those associated with the largest eigenvalue.

In addition, it is possible to include past values of EMG data to be linearly combined by the filter, in order to increase further the SCR. This means including also delayed signals in the sum operations in the definition of the SCR given by Equation (1). This way, both a spatial and a temporal filter are applied. To get the optimal combination of weights, the solution described above is still valid: the only difference is that additional signals (i.e., the delayed versions of EMG data) are included. The optimal spatio-temporal filter (OSTF) is thus obtained.

A tuning of the delay between subsequent samples (in the range of 1 to 10) and temporal filter order (up to 5) have been conducted on a validation dataset (i.e., a portion of data different from the training one, as detailed below), with the aim to get maximal SCR and avoid over-fitting.

Notice that delayed data could have a high mutual correlation, which implies a great condition number of autocorrelation matrices R_S and R_C. That is true especially if the delay is small and the length of the temporal filter is large. To avoid this problem, the autocorrelation matrices have been regularized as

$$\widehat{R}_S = R_S + 10^{-4}\lambda_{max}^S I \quad (7)$$

$$\widehat{R}_C = R_C + 10^{-4}\lambda_{max}^C I \quad (8)$$

where λ_{max}^S and λ_{max}^C are the maximum eigenvalues of the matrices R_S and R_C, respectively, and I is the identity matrix.

In this way, the maximum conditional number has been set in the order of 10^4.

B. EXPERIMENTAL PROTOCOL

Two muscles have been studied in this work: PT and FCR. They are placed anatomically one close to the other in the distal part of the arm (see Fig. 1(a)) and their contractions enable different movements of the wrist: pronation and flexion, respectively. Because of their anatomical proximity, the issue of crosstalk is relevant in EMG acquisitions, determining a bias in the estimation of amplitude and spectral indexes.

Selective isotonic and isometric contractions of the target and crosstalk muscles have been obtained through a specific instrument designed and realized for this study, shown in Fig. 1(b). It consists of a forearm support, to which two plates are connected, forming a 'handle' in which the hand is inserted. The wrist is immobilized through bands fixed to the instrument. The physical connection between the elements has been obtained through two load cells (manufacturer Hxastlp, model TAL220, capacity of 20 kg), which quantify the forces applied to the handle during the experiment.

Analog signals produced by the previous sensors were amplified, sampled at 10 Hz and digitalized with a 24-bit ADC (through two acquisition boards HX711 by OOTDTY, one for each transductor). The resulting digital signal was then processed through an Arduino® UNO board. The electrical connections between the previous components are reported in Fig. 1(c). Signals were then sent to a workstation (2.3 GHz, dual-core CPU and 8-GB of RAM),

that processed the acquired data through MATLAB®. Since each load cell produces a signal depending on its deformation, this experimental set-up allows to distinguish flexion and pronation of the wrist analyzing the phase of signals produced. Indeed, when a flexion occurs their ideal phase is 0, whereas during a twist the phase is 180 degrees.

Eight healthy volunteers (six males and two females; mean±standard deviation: age 28.1±7.5 years, height 176.8±7 cm, weight 71±11.2 kg) participated in this study. The experiments were conducted in the venues of the University of Turin, and in accordance with the Declaration of Helsinki. The study was approved by the Ethical Committee of the University of Turin (approval number 510190).

Before electrode placement, the muscles of interest were identified by palpation during a selective contraction. The skin was then slightly abraded with abrasive paste and a matrix of electrodes (13 rows and 5 columns) with inter-electrode distance (IED) of 8 mm was placed with the long side inclined about 45 degrees to the forearm, assuming that two columns were over the pronator teres (PT), two on the flexor carpi radialis (FCR) and the central one in between, as shown in Fig. 1(a). Then instructions on the experiment were given to each subject and some free trials were made. During the experiment, visual force feedback was provided to the subject, representing the average of the absolute readings of the load cells. Since this signal needed to be provided as additional input to the EMG amplifier (Quattrocento, OT Bioelettronica, Turin, Italy), including software for visual feedback, a new digital-to-analog conversion was executed. Specifically, the analog signal was obtained by filtering the pulse-width modulation (PWM) wave, generated from the D9 pin of the Arduino® UNO board, through a second-order low pass filter, with cut off frequency of 10 Hz.

The experimental protocol, briefly summarised in Fig. 1(d), included the acquisitions of three maximal voluntary contractions (MVC) and a series of submaximal contractions for each muscle. Monopolar signals were acquired during the experiment choosing as reference one electrode placed on the elbow. Each subject performed the MVCs for 5 s, with a rest of 120 s between them. The highest value among MVCs was chosen as valid. Then, two sets of exercises were requested from the subjects, consisting of five isometric contractions of PT and FCR, as selective as possible, at different force levels: from 10% to 50% MVC of the respective muscle, each lasting 20 s. Between the acquisitions, a rest of 60 s has been observed. The order of force levels for the tasks was determined randomly, to avoid cumulative effects. The EMG signals were then amplified, band-pass filtered (-3 dB bandwidth, 10-500 Hz), sampled at 2048 Hz, and converted to digital form with a resolution of 16-bit. During the experiments we monitored the phase of the signals produced by the load cells and the acquisitions that did not meet the phase requirements (0° and 180° during flexion and pronation, respectively) were repeated.

C. OSTF PERFORMANCE TESTS

The performance of the OSTF was assessed in different conditions and compared to those of traditional spatial filters. The following parameters were varied:

- The source of input (only in case of small electrodes): SD or DD.
- The selectivity of the acquisition, depending on the type of electrodes. Either small physical electrodes or large square electrodes (simulated by summing the potentials from more physical electrodes) were considered, the first with an IED of 8 mm, and the latter with an IED of 16 mm.
- The duration of the epochs used for training the OSTF; starting from 125 ms to 2000 ms doubling at each step the temporal length of the signal.

In order to work on stationary data, the first and last 5 seconds of the recordings were discarded; indeed, during the first seconds of acquisition, the subject reached the force level to be studied, while during the final ones, there could be variations due to fatigue (possibly reducing the selectivity of the contractions). Therefore, the central 10 seconds of each contraction were considered.

The data provided during the training phase were obtained by concatenating epochs at increasing force levels. The epochs were 2 seconds long as default and shorter when investigating the effect of the train duration on the performances of the OSTF. The validation set, through which the tunings of delay and filter order have been conducted, was created with the same structure and temporal length of epochs concatenated. The remaining EMGs were used as a test set, to evaluate the performances of the OSTF.

Different levels of crosstalk have been simulated, by summing EMG epochs of the crosstalk muscle to the selective contraction of PT at specific force levels. This could be considered as an approximate simulation of the co-contraction of the two muscles: from the physiological viewpoint, there are problems, as a real co-contraction would encompass sensory feedback that would couple the activities of the two muscles; however, from the technical viewpoint, the ability of a filter to reduce crosstalk is not related to the specific recruitment of MUs, so that we expect that reliable information can be obtained from our tests. In this way, different SCRs could be simulated. Moreover, we could use as reference the original signals (i.e., those obtained from the selective contractions of PT), comparing the amplitude and spectral indexes extracted before and after corrupting them with crosstalk EMGs. The average rectified value (ARV) was used as the amplitude indicator and the median frequency (MDF) was selected as the spectral index, both estimated in epochs of 0.5 s.

D. STATISTICAL ANALYSIS

The percentage errors (i.e., absolute of difference with respect to crosstalk-free condition) of ARV and MDF of EMGs recorded over PT were estimated considering the sum of crosstalk signals from FCR at different contraction
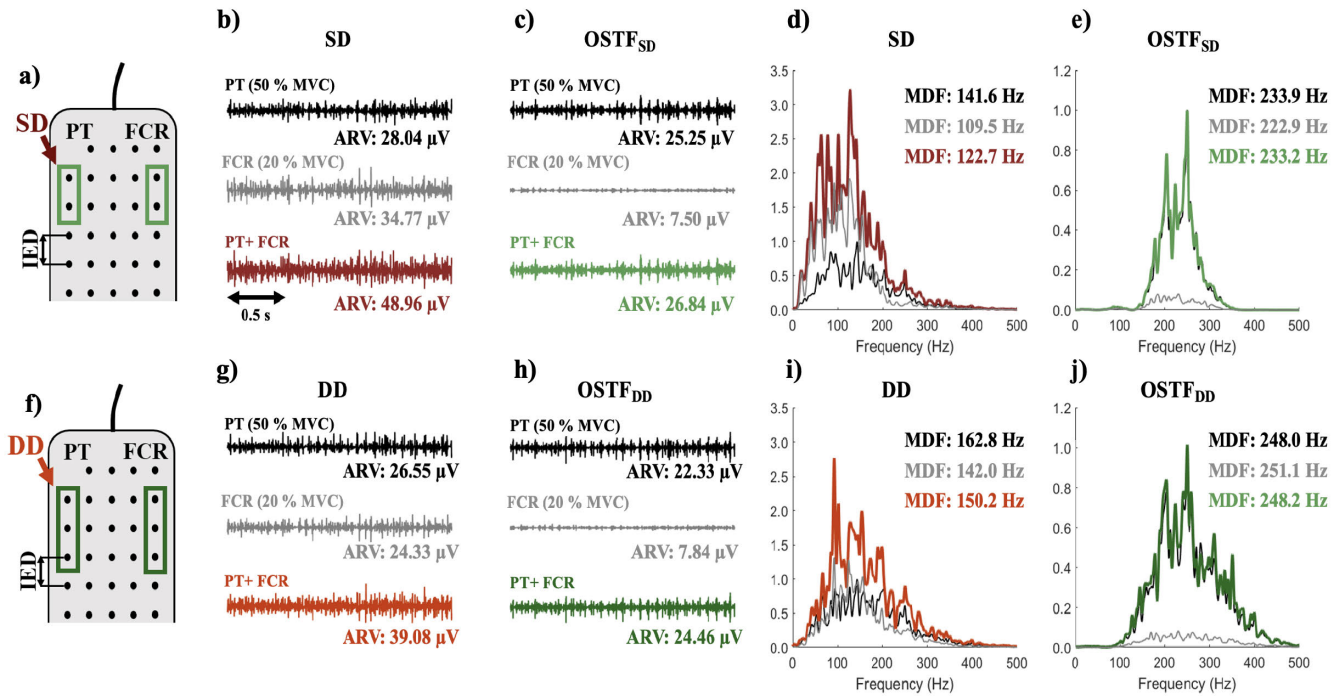
FIGURE 2. Signals recorded over PT using small electrodes with IED of 8 mm and produced by the contractions of PT (50 % MVC) and FCR (20 % MVC). The sum of the two signals (PT+FCR) is also shown as a simulation of a signal corrupted by crosstalk. On the right side of the image, the power spectral densities (PSDs, estimated by Welch method, considering sub-epochs of 0.5 s, overlap of 50% and zero padding to get 0.5 Hz resolution; they are normalized with respect to the maximum of the PSD of the EMG of PT) are shown. ARV and MDF of the signals are reported. a) Electrodes chosen for estimating the two single differential (SD) signals. The channels included in the light green boxes are used for determining the SDs provided to OSTF as input. The coloured arrow indicates which SD was used for the comparison in b) and d). b) Single differential signals. c) Output of OSTF obtained with SD signals (OSTF$_{SD}$ configuration). d) PSD and MDF of the signals reported in b). e) PSD and MDF of the signals shown in c). f)-j) Same as a)-e) (respectively), but considering DD signals for both the comparison and source for OSTF (OSTF$_{DD}$ configuration).
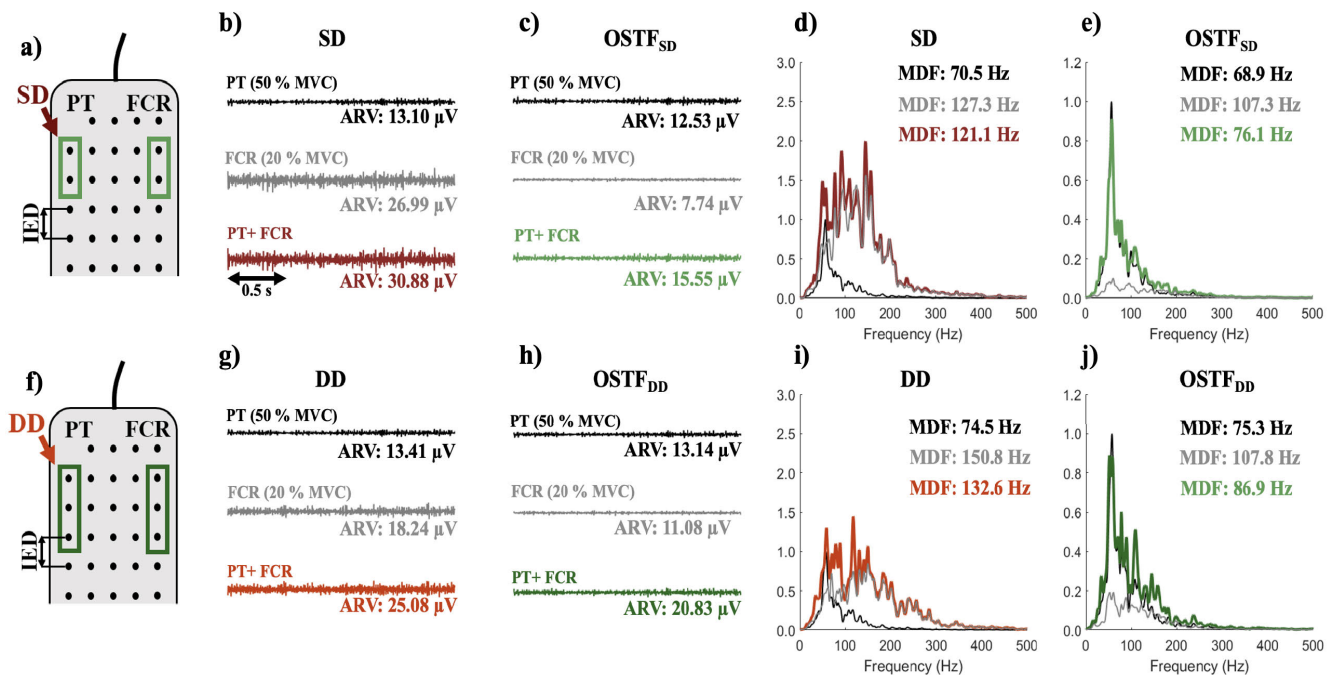
FIGURE 3. Same as Fig. 2, but considering a signal from another subject.

levels. We conducted a series of repeated measure three-way ANOVAs for ARV and MDF percentage errors with filter

(source vs OSTF, trained with the same source), target force level (10, 20, 30, 40, and 50 %), level of crosstalk (10, 20, 30,

40 and 50 %) as within-subject factors. We also investigated the effect of training time (125, 250, 500, 1000 and 2000 ms) on ARV and MDF percentage errors. More specifically, we conducted three separate ANOVAs through the software JASP (JASP Team, Version 0.17.3):

1) OSTF based on selective SD channels (indicated with $OSTF_{SD}$) compared with selective SD signals,
2) OSTF using selective DD channels as inputs (indicated with $OSTF_{DD}$) compared with DD signals,
3) OSTF applied to not-selective SD channels, i.e., with large electrodes and IED (indicated with $OSTF_{SD}^{LE}$) compared to not-selective SD data (labelled as SD^{LE}).

The Greenhouse-Geisser correction was adopted when sphericity was violated. The effect size was determined using partial η^2.

III. RESULTS

Examples of signals from two subjects and power spectral densities (PSD) are shown in Fig. 2 and 3. EMGs filtered by the OSTF (using either SD or DD as input source) are compared with those recorded by SD and DD channels placed over the target muscle, both in the presence and absence of crosstalk. More specifically, SDs were obtained by combining the first two electrodes in the light green boxes of Fig. 2(a), while DDs were estimated considering the first three electrodes in the dark green boxes of Fig. 2(b). Processing the SD signals recorded from the two muscles by the OSTF, the $OSTF_{SD}$ was obtained; using the DDs, the $OSTF_{DD}$ was developed. The activity of PT at 50% MVC has been corrupted with a contraction of FCR at 20% MVC, to simulate crosstalk. The OSTF shows a better rejection of crosstalk with respect to the other filters in both cases, reducing the bias in estimating both amplitude and spectral properties. Comparing the PSDs obtained with the OSTFs in Fig. 2(e) and 2(j) and Fig. 3(e) and 3(j), it is possible to appreciate the ability of the filter of emphasizing the bandwidth of the signals where the SCR is higher, in order to suppress crosstalk; in the two considered subjects, the selected bandwidths are very different.

Fig. 4 shows the effect of crosstalk on the estimation of amplitude and spectral features from data recorded using different filters. In this figure, all the subjects participating in the experiment were considered. The performances were evaluated in terms of the percentage absolute difference with respect to the ARV and MDF estimated on the original EMG of the PT without the corruption given by adding the crosstalk from the FCR. Different acquisition conditions are considered, with small and large electrodes. As a reminder, the big square electrodes have been simulated by summing potentials from 4 physical electrodes and doubling the IED (see the inner scheme of Fig. 4(c)). The OSTF has been developed using the spatial filters to which it is compared: either SD ($OSTF_{SD}$) or DD ($OSTF_{DD}$) from small electrodes, or the bipolar detection with large electrodes ($OSTF_{SD}^{LE}$), using one channel from each muscle (i.e., the target

and the crosstalk muscle). Concerning the small electrode configuration, the percentage errors in ARV estimation were 157.30±57.11 % (mean±std), 38.54±10.47 % for SD and $OSTF_{SD}$, respectively; percentage errors of 131.67±47.16 % and 39.39±8.47 % were obtained considering DD and $OSTF_{DD}$ configurations, respectively. As regards MDF, we obtained an estimation error of 23.57±3.92 % and 8.31±0.88 % for SD and $OSTF_{SD}$ conditions, whereas they were 20.20±1.21 % and 12.46±0.96 % when considering DD and $OSTF_{DD}$, respectively. In the case of large simulated electrodes, the percentage errors in ARV estimation were 243.22±86.73 % and 70.84±26.75 %, for SD^{LE} and $OSTF_{SD}^{LE}$, respectively. Moreover, we obtained the following percentage errors in the estimation of MDF for the SD^{LE} and $OSTF_{SD}^{LE}$ configurations: 18.59±3.28 % and 10.20±0.96 %.

The details of the statistical analysis are reported in Table 1. Notice that the error is always reduced by using the OSTF, with statistically significant differences with respect to using the classical filters in all conditions except for two cases: MDF with DD and ARV when using large electrodes (however, in this latter case, notice that the interaction of "Filter x Crosstalk" has $p = 0.050$, reflecting an improvement when the crosstalk level is high).

Fig. 5 investigates the effect of the duration of the signals used for training the OSTF. The same configurations of electrodes (small and large) and filters (SD and DD) as before were considered. The OSTFs were trained considering concatenated signal epochs of different durations: 125, 250, 500, 1000 and 2000 ms, respectively. The percentage errors in estimating ARV and MDF are shown. Table 2 reports the detailed statistical analysis. The statistics show that reducing the duration of the signal used for training has only marginal effects, which are not statistically significant. Therefore, the OSTF can be trained even with signals lasting hundreds of ms, still guaranteeing a low bias due to crosstalk in ARV and MDF estimation.

IV. DISCUSSION

Crosstalk is an undesired contribution due to the contraction of adjacent muscles that may occur when EMG is acquired over a target muscle of interest [9], [12], [32], [37]. Nowadays there are several methods to attenuate crosstalk [21], [27], [29], [30], [34], [37]; however, simple ones (both in terms of the recording system and data processing) are preferred in applications; for this reason, the most popular approach consists in using spatial filters [18], [20]. Indeed, with a linear combination of signals recorded over the target muscle (e.g., in SD or DD configuration), it is possible to reduce crosstalk, with the compromise that only a small detection volume is considered. However, this solution is not optimal in all conditions. In fact, the performances of those filters are strongly influenced by subject anatomy [13]; moreover, selective spatial filters decrease the amount of crosstalk by reducing the detection volume, so that they explore only a small portion of the target muscle and the activity of the MUs included into it may not actually be representative of
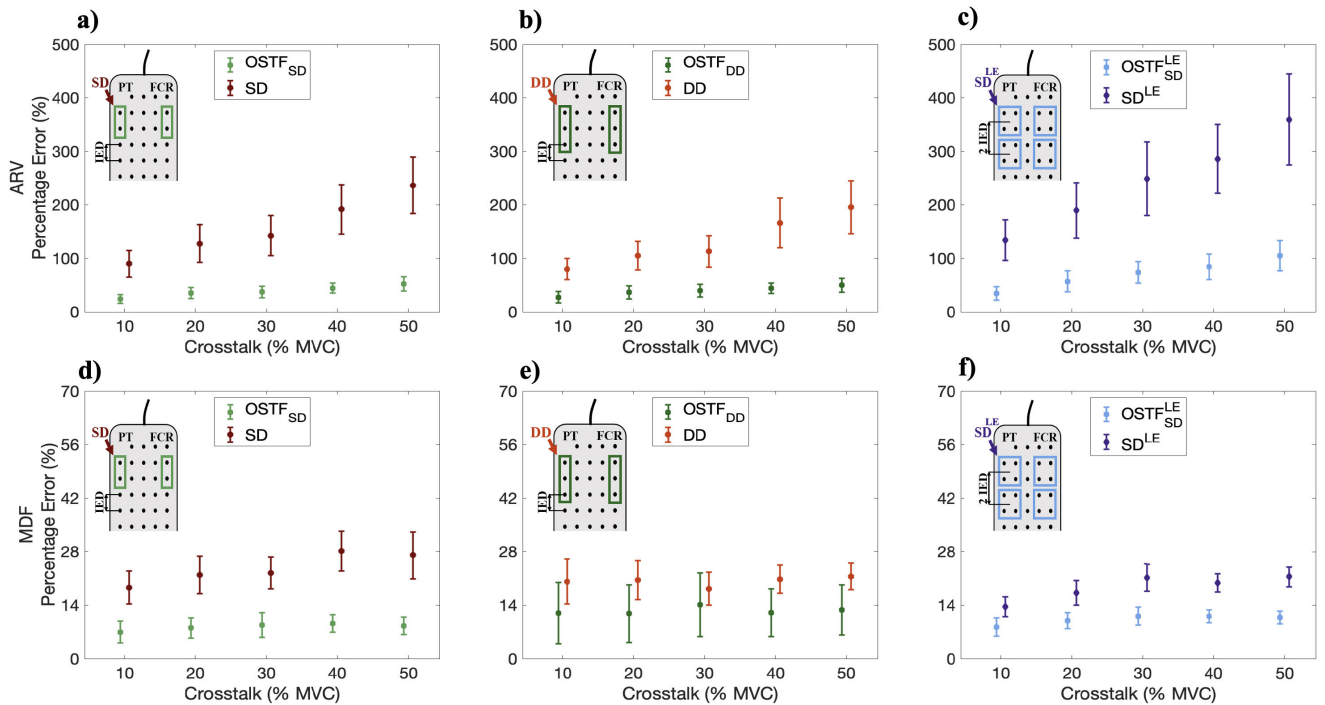
FIGURE 4. Percentage error (i.e., absolute of difference with respect to crosstalk-free condition) in ARV and MDF estimations with different filters and levels of crosstalk (from 10% to 50% MVC). OSTF has been applied to different sources to evaluate the behaviour of the method in different conditions of acquisition. In each figure, OSTF has been compared with the source recorded over PT (indicating with an arrow of a different colour the channels for obtaining it). a) Percentage error in ARV estimation using the detection system recording an SD channel over the PT and another over the FCR, obtained using physical electrodes with IED of 8 mm (OSTF$_{SD}$ configuration). b) Percentage error in ARV estimation using the detection system recording a DD channel over the PT and another over the FCR, obtained using physical electrodes with IED of 8 mm (OSTF$_{DD}$ configuration). c) Percentage error in ARV estimation using the detection system recording an SD channel over the PT and another over the FCR, obtained using large electrodes (simulated as the sum of the potentials from 4 physical electrodes) with IED of 16 mm (OSTF$_{SD}^{LE}$ configuration). d) Error in MDF estimation using the detection configuration in a). e) Error in MDF estimation using the detection configuration in b). f) Error in MDF estimation using the detection configuration in c).

TABLE 1. Statistical analysis results for Fig. 4. The factor "Filter" and the interactions "Filter x Target Force Level" (abbreviated as "Filter x Target"), "Filter x Crosstalk", and "Filter x Target x Crosstalk" are reported. The table has been divided into two parts, for ARV and MDF estimation errors, respectively. The OSTF$_{SD}$ - SD condition is relative to Fig. 4 (a) and (d), the OSTF$_{DD}$ - DD condition is associated to Fig. 4 (b) and (e), while the OSTF$_{SD}^{LE}$ - SD^{LE} combination is relative to Fig. 4 (c) and (f). Bold values in the table indicate statistically significant differences ($p < 0.05$).

| | ARV | | | | | | | | | MDF | | | | | | | | |
| | OSTF$_{SD}$ - SD | | | OSTF$_{DD}$ - DD | | | OSTF$_{SD}^{LE}$ - SD^{LE} | | | OSTF$_{SD}$ - SD | | | OSTF$_{DD}$ - DD | | | OSTF$_{SD}^{LE}$ - SD^{LE} | | |
	F	p	η^2	F	p	η^2	F	p	η^2	F	p	η^2	F	p	η^2	F	p	η^2
Filter	11.7	**0.014**	0.661	8.3	**0.028**	0.582	5.7	0.053	0.490	7.1	**0.037**	0.544	0.5	0.472	0.089	6.0	**0.050**	0.501
Filter x Target	9.0	**0.012**	0.601	4.8	**0.048**	0.448	3.0	0.129	0.334	0.4	0.531	0.072	1.2	0.315	0.168	0.4	0.603	0.061
Filter x Crosstalk	19.2	**<0.001**	0.762	7.6	**0.025**	0.561	5.2	**0.050**	0.469	1.9	0.201	0.245	0.7	0.572	0.110	2.0	0.114	0.258
Filter x Target x Crosstalk	14.3	**<0.001**	0.705	5.1	**<0.001**	0.459	2.4	**0.004**	0.287	0.5	0.904	0.086	1.1	**0.002**	0.159	0.4	0.967	0.069

the entire muscle [28]. Furthermore, if the recording system has a great IED, the selectivity of the filters decreases and crosstalk may be included [13].

In this study, we experimentally evaluated a method that can overcome most of the limitations presented above. Indeed, the OSTF has been meant to emphasize the EMG reflecting the activity of the target muscle, while discarding that of adjacent muscles, adapting to the anatomy of the subject. The method is data-driven and could work regardless of the type of recording system used.

The core of the method consists of a training phase, in which selective contractions of target and crosstalk

muscles are considered. During this phase, the linear combination of signals defining the filter is chosen to maximize the SCR; the filter weights take into account both the anatomy (that we suppose as constant since data were recorded in the same conditions during the experimental protocol) and spatial-temporal recruitment of the MUs involved during the selective contractions. The optimization problem that characterizes the training phase guarantees that the filter is optimal on such data (in the mean squared sense). Therefore, problems may occur if EMGs provided to the filter differ consistently from the ones used for training. However, if the volume conductor and the recording system
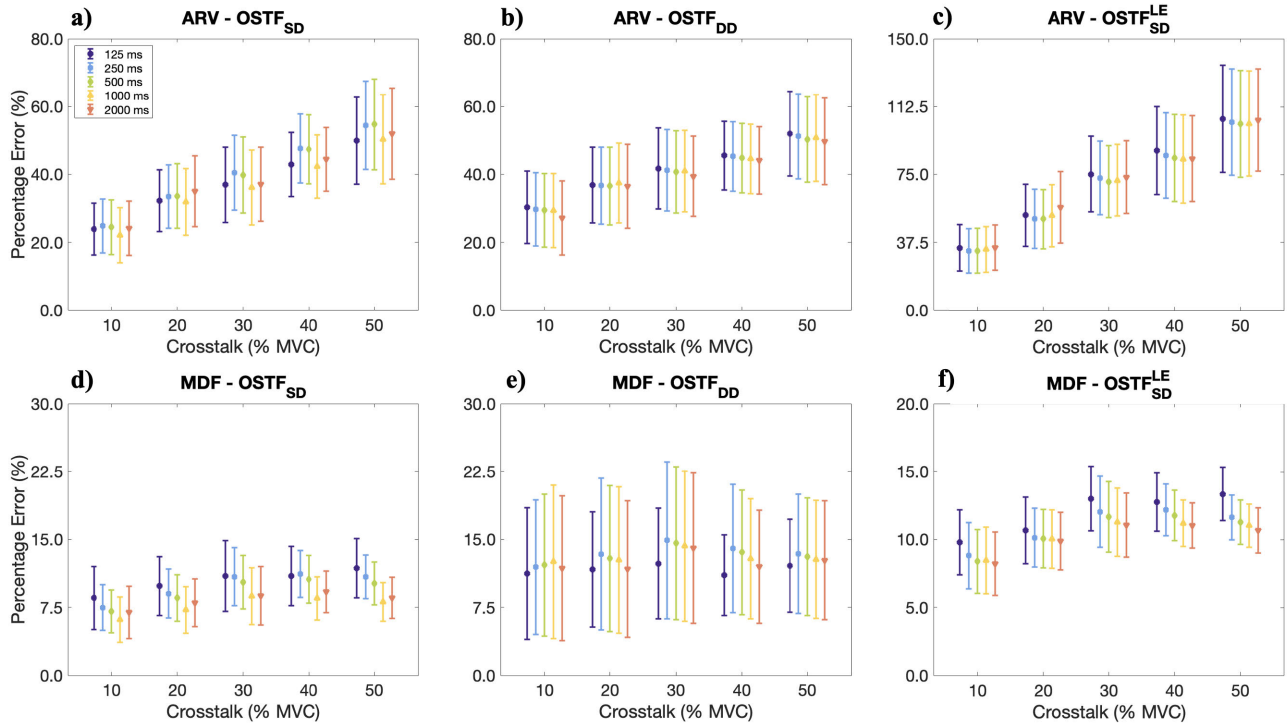
FIGURE 5. Percentage error in ARV (a-b-c) and MDF (d-e-f) estimation, varying the levels of crosstalk and different temporal length of the signal used to train the OSTF. Different temporal lengths have been explored: 125, 250, 500, 1000 and 2000 ms, respectively. In addition, various sources provided as input to OSTF were considered: SD and DD obtained with small electrodes (OSTF$_{SD}$ and OSTF$_{DD}$ conditions) and SD^{LE} obtained through large sensors (OSTF$_{SD}^{LE}$).

TABLE 2. Statistical analysis of the results of Fig. 5. The factor "Timing" and the interactions "Timing x Target Force Level" (abbreviated as "Timing x Target"), "Timing x Crosstalk", and "Timing x Target x Crosstalk" are reported. The table has been divided into two parts, for ARV and MDF estimation errors respectively. The OSTF$_{SD}$ - SD condition is relative to Fig. 5 (a) and (d), the OSTF$_{DD}$ - DD condition is associated to Fig. 5 (b) and (e), while the OSTF$_{SD}^{LE}$ - SD^{LE} one is relative to Fig. 5 (c) and (f). Bold values in the table indicate statistically significant differences ($p < 0.05$).

| | ARV | | | | | | | | | MDF | | | | | | | | |
| | OSTF$_{SD}$ - SD | | | OSTF$_{DD}$ - DD | | | OSTF$_{SD}^{LE}$ - SD^{LE} | | | OSTF$_{SD}$ - SD | | | OSTF$_{DD}$ - DD | | | OSTF$_{SD}^{LE}$ - SD^{LE} | | |
	F	p	η^2	F	p	η^2	F	p	η^2	F	p	η^2	F	p	η^2	F	p	η^2
Timing	0.6	**0.468**	0.003	0.3	0.605	0.059	3.4	0.072	0.001	1.1	0.333	0.162	0.6	0.505	0.103	3.4	0.096	0.016
Timing x Target	0.7	0.744	0.002	10.6	**<0.001**	0.639	1.5	0.085	0.001	0.9	0.571	0.131	0.8	0.425	0.132	2.2	**0.007**	0.016
Timing x Crosstalk	0.8	0.626	0.001	0.2	1.000	0.032	0.9	0.571	0.001	1.2	0.265	0.169	0.4	0.665	0.078	0.6	0.852	0.002
Timing x Target x Crosstalk	0.7	0.925	0.001	2.4	**<0.001**	0.290	1.0	0.457	0.001	1.1	0.160	0.166	1.0	0.202	0.112	0.7	0.903	0.008

are maintained constant, the performances of the filter should be stable: indeed, simulations indicated that only marginal decrements of OSTF performances were observed by activating new MUs only in the generation of the test signals or considering myoelectric fatigue effects only during the test [32]. Thus, we can expect that problems can arise only if there are important changes in recorded data: for example, this could happen in dynamic contractions if the range of movement varies during the test or in the case in which the electrode contact impedance changes drastically. However, in the present study, isometric and iso-tonic contractions in controlled conditions were considered, thus avoiding those problematic situations (left for future studies).

In order to avoid overfitting, the lag between delayed data and the order of the temporal filter were tuned on a different dataset (validation set).

Different acquisition modalities have been considered for the validation of OSTF: using small electrodes placed close to each other (IED of 8 mm, see Figure 4 (a) and (b)), or large electrodes (simulated by summing the potentials from 4 electrodes in the matrix), where the IED became 16 mm (see Figure 4 (c)). Therefore, according to the source used, we obtained three configurations: OSTF$_{SD}$ and OSTF$_{DD}$ for small electrodes and OSTF$_{SD}^{LE}$ for large ones.

We acquired the EMGs at different force levels of two muscles: PT and FCR. We expect that the acquired contractions were not perfectly selective, especially at high

levels of force (40 and 50 % MVC). However, this does not prevent the application of our method. In fact, OSTF can provide superior SCRs than those of SD and DD even in these conditions [32]. Concerning the spectral estimation, OSTF is less sensible to crosstalk, as reported in Fig.2 and 3. Notice that the bandwidth of OSTF output can be much different from those of SD and DD; that is because OSTF empathizes the (subject-specific) band of frequencies where the signal prevails over crosstalk.

Two EMG indexes (ARV and MDF) were estimated through OSTF outputs and compared with those obtained from SD and DD. The estimation of these indexes was compared when applied to the original signals or to those obtained by adding the crosstalk with different levels. The differences between filters in ARV estimation increase with the level of crosstalk, regardless of the modality of acquisition, i.e., considering small electrodes area or big square sensors with a double IED, as reported in Fig. 4 (a), (b) and (c). Significant improvements have been recorded also in MDF estimation when using SD signals (see Fig. 4 (d) and (f)), whereas the mean improvement observed when comparing with DD was not significant (Fig. 4 (e); this is possibly due to the small size of our sample; however, when increasing the contraction level of the crosstalk muscle, the improvement of the OSTF was more evident, showing that its usefulness emerges in difficult conditions).

The duration of the epochs used to train the OSTF is an important feature to be considered. Results show that it does not influence much the performances in the estimation of EMG indexes (at least if the duration is reasonable: the shortest considered epochs were 125 ms long). Therefore, the training and tuning phases can be conducted rapidly and with a few seconds of signals. This result is particularly significant if only few selective contractions are available.

In conclusion, the OSTF provides good rejection of crosstalk, without penalizing the information recorded from the target muscle. It needs only a few seconds of signals for the training. It can be applied even with a single channel over each muscle of interest (one channel over the target and one on the crosstalk muscle were considered here). Therefore, the method can find several applications in conditions in which simple detection systems are applied (e.g., from gesture recognition [38] to gait cycle analysis [25]) employing few electrodes and classical spatial filtering.

As a limitation, our study includes a small dataset, that could be increased in the future. Moreover, further works may be focused on assessing the performance of the method when dynamic contractions are executed, since here only isometric conditions were evaluated. Fatiguing contractions could also be studied (even if simulations provided in [32] already provide some confidence that the method is not much affected by myoelectric fatigue). Moreover, changes in the tuning phases may be taken into consideration. For example, if the user is interested in a specific EMG index, the tuning phase may be focused on selecting parameters which reduce its estimation error in the presence of crosstalk. Finally,

an alternative strategy of training can be adopted, e.g., a force ramp contraction for each muscle instead of concatenating EMGs at increasing force levels.

V. CONCLUSION
In this paper, we experimentally validated a method to reduce crosstalk in surface EMG based on an optimal spatio-temporal filter (OSTF) adapted to the subject. It requires a training phase in which few seconds of (even not perfectly) selective contractions can be used. The performances of ARV and MDF estimations are influenced by the detection system, the level of crosstalk and the type of input signals (SD or DD); however, they are always superior to spatial filters used to record the data. Moreover, good performances are achieved even when the duration of the data used for training is very short (in the order of hundreds of ms). The method can be applied in real-time conditions and employed even with data recorded with few electrodes placed on target and crosstalk muscles.

REFERENCES
[1] G. R. Naik, D. K. Kumar, and M. Palaniswami, "Signal processing evaluation of myoelectric sensor placement in low-level gestures: Sensitivity analysis using independent component analysis," *Expert Syst.*, vol. 31, no. 1, pp. 91–99, Feb. 2014.

[2] M. Besomi et al., "Consensus for experimental design in electromyography (CEDE) project: Electrode selection matrix," *J. Electromyogr. Kinesiol.*, vol. 48, pp. 128–144, Oct. 2019.

[3] A. Péter, E. Andersson, A. Hegyi, T. Finni, O. Tarassova, N. Cronin, H. Grundström, and A. Arndt, "Comparing surface and fine-wire electromyography activity of lower leg muscles at different walking speeds," *Frontiers Physiol.*, vol. 10, p. 1283, Oct. 2019.

[4] A. Merlo, M. C. Bò, and I. Campanini, "Electrode size and placement for surface EMG bipolar detection from the brachioradialis muscle: A scoping review," *Sensors*, vol. 21, no. 21, p. 7322, Nov. 2021.

[5] I. Campanini, A. Merlo, C. Disselhorst-Klug, L. Mesin, S. Muceli, and R. Merletti, "Fundamental concepts of bipolar and high-density surface EMG understanding and teaching for clinical, occupational, and sport applications: Origin, detection, and main errors," *Sensors*, vol. 22, no. 11, p. 4150, May 2022.

[6] E. A. Clancy, E. L. Morin, G. Hajian, and R. Merletti, "Tutorial. Surface electromyogram (sEMG) amplitude estimation: Best practices," *J. Electromyogr. Kinesiol.*, vol. 72, Oct. 2023, Art. no. 102807.

[7] I. Talib, K. Sundaraj, C. K. Lam, J. Hussain, and M. A. Ali, "A review on crosstalk in myographic signals," *Eur. J. Appl. Physiol.*, vol. 119, no. 1, pp. 9–28, Jan. 2019.

[8] K. M. Barr, A. L. Miller, and K. B. Chapin, "Surface electromyography does not accurately reflect rectus femoris activity during gait: Impact of speed and crouch on vasti-to-rectus crosstalk," *Gait Posture*, vol. 32, no. 3, pp. 363–368, Jul. 2010.

[9] N. Jiang, K. B. Englehart, and P. A. Parker, "Extracting simultaneous and proportional neural control information for multiple-DOF prostheses from the surface electromyographic signal," *IEEE Trans. Biomed. Eng.*, vol. 56, no. 4, pp. 1070–1080, Apr. 2009.

[10] J. Zhao, Y. Yu, X. Wang, S. Ma, X. Sheng, and X. Zhu, "A musculoskeletal model driven by muscle synergy-derived excitations for hand and wrist movements," *J. Neural Eng.*, vol. 19, no. 1, Feb. 2022, Art. no. 016027.

[11] N. Zhao, B. Zhao, G. Shen, C. Jiang, Z. Wang, Z. Lin, L. Zhou, and J. Liu, "A robust HD-sEMG sensor suitable for convenient acquisition of muscle activity in clinical post-stroke dysphagia," *J. Neural Eng.*, vol. 20, no. 1, Feb. 2023, Art. no. 016018.

[12] K. Yong-Ku, M. S. Hallbeck, and J. Myung-Chul, "Crosstalk effect on surface electromyogram of the forearm flexors during a static grip task," *J. Electromyogr. Kinesiol.*, vol. 20, no. 6, pp. 1223–1229, 2010.

[13] L. Mesin, S. Smith, S. Hugo, S. Viljoen, and T. Hanekom, "Effect of spatial filtering on crosstalk reduction in surface EMG recordings," *Med. Eng. Phys.*, vol. 31, no. 3, pp. 374–383, 2009.

[14] N. S. Stoykov, M. M. Lowery, and T. A. Kuiken, "A finite-element analysis of the effect of muscle insulation and shielding on the surface EMG signal," *IEEE Trans. Biomed. Eng.*, vol. 52, no. 1, pp. 117–121, Jan. 2005.

[15] L. Mesin, "Simulation of surface EMG signals for a multilayer volume conductor with a superficial bone or blood vessel," *IEEE Trans. Biomed. Eng.*, vol. 55, no. 6, pp. 1647–1657, Jun. 2008.

[16] M. M. Lowery, N. S. Stoykov, A. Taflove, and T. A. Kuiken, "A multiple-layer finite-element model of the surface EMG signal," *IEEE Trans. Biomed. Eng.*, vol. 49, no. 5, pp. 446–454, May 2002.

[17] M. M. Lowery, N. S. Stoykov, J. P. A. Dewald, and T. A. Kuiken, "Volume conduction in an anatomically based surface EMG model," *IEEE Trans. Biomed. Eng.*, vol. 51, no. 12, pp. 2138–2147, Dec. 2004.

[18] C. J. De Luca, M. Kuznetsov, L. Gilmore, and S. Roy, "Inter-electrode spacing of surface EMG sensors: Reduction of crosstalk contamination during voluntary contractions," *J. Biomech.*, vol. 45, pp. 555–561, Feb. 2011.

[19] D. Farina, R. Merletti, B. Indino, M. Nazzaro, and M. Pozzo, "Surface EMG crosstalk between knee extensor muscles: Experimental and model results," *Muscle Nerve*, vol. 26, no. 5, pp. 681–695, 2002.

[20] D. Farina, L. Arendt-Nielsen, R. Merletti, B. Indino, and T. Graven-Nielsen, "Selectivity of spatial filters for surface EMG detection from the tibialis anterior muscle," *IEEE Trans. Biomed. Eng.*, vol. 50, no. 3, pp. 354–364, Mar. 2003.

[21] D. Farina, C. Fevotte, C. Doncarli, and R. Merletti, "Blind separation of linear instantaneous mixtures of nonstationary surface myoelectric signals," *IEEE Trans. Biomed. Eng.*, vol. 51, no. 9, pp. 1555–1567, Sep. 2004.

[22] R. Merletti, C. J. De Luca, and D. Sathyan, "Electrically evoked myoelectric signals in back muscles: Effect of side dominance," *J. Appl. Physiol.*, vol. 77, pp. 2104–2114, Jan. 1994.

[23] M. Lowery, N. Stoykov, and T. Kuiken, "A simulation study to examine the use of cross-correlation as an estimate of surface EMG cross talk," *J. Appl. Physiol.*, vol. 94, pp. 1324–1334, May 2003.

[24] N. A. Dimitrova, G. V. Dimitrov, and O. A. Nikitin, "Neither high-pass filtering nor mathematical differentiation of the EMG signals can considerably reduce cross-talk," *J. Electromyogr. Kinesiol.*, vol. 12, no. 4, pp. 235–246, Aug. 2002.

[25] I. Campanini, A. Merlo, P. Degola, R. Merletti, G. Vezzosi, and D. Farina, "Effect of electrode location on EMG signal envelope in leg muscles during gait," *J. Electromyogr. Kinesiol.*, vol. 17, pp. 515–526, May 2007.

[26] L. Mesin, "Separation of interference surface electromyogram into propagating and non-propagating components," *Biomed. Signal Process. Control*, vol. 52, pp. 238–247, Jul. 2019.

[27] L. Mesin, "Inverse modelling to reduce crosstalk in high density surface electromyogram," *Med. Eng. Phys.*, vol. 85, pp. 55–62, Nov. 2020.

[28] T. M. Vieira, A. Botter, S. Muceli, and D. Farina, "Specificity of surface EMG recordings for gastrocnemius during upright standing," *Sci. Rep.*, vol. 7, no. 1, p. 13300, Oct. 2017.

[29] L. Mesin, "Real time identification of active regions in muscles from high density surface electromyogram," *Comput. Biol. Med.*, vol. 56, pp. 37–50, Jan. 2015.

[30] C. M. Germer, D. Farina, L. A. Elias, S. Nuccio, F. Hug, and A. D. Vecchio, "Surface EMG cross talk quantified at the motor unit population level for muscles of the hand, thigh, and calf," *J. Appl. Physiol.*, vol. 131, no. 2, pp. 808–820, Aug. 2021.

[31] C. Chen, Y. Yu, X. Sheng, D. Farina, and X. Zhu, "Simultaneous and proportional control of wrist and hand movements by decoding motor unit discharges in real time," *J. Neural Eng.*, vol. 18, no. 5, Oct. 2021, Art. no. 056010.

[32] L. Mesin, "Optimal spatio-temporal filter for the reduction of crosstalk in surface electromyogram," *J. Neural Eng.*, vol. 15, no. 1, Feb. 2018, Art. no. 016013.

[33] Z. J. Koles, M. S. Lazar, and S. Z. Zhou, "Spatial patterns underlying population differences in the background EEG," *Brain Topogr.*, vol. 2, no. 4, pp. 275–284, 1990.

[34] A. Magbonde, F. Quaine, and B. Rivet, "Comparison of blind source separation methods to surface electromyogram for extensor muscles of the index and little fingers," in *Proc. 44th Annu. Int. Conf. IEEE Eng. Med. Biol. Soc. (EMBC)*, Jul. 2022, pp. 3615–3618.

[35] I. K. Niazi, N. Jiang, O. Tiberghien, J. F. Nielsen, K. Dremstrup, and D. Farina, "Detection of movement intention from single-trial movement-related cortical potentials," *J. Neural Eng.*, vol. 8, no. 6, Oct. 2011, Art. no. 066009.

[36] R. Fletcher, *Practical Methods of Optimization*. New York, NY, USA: Wiley, 1987.

[37] L. Mesin, "Crosstalk in surface electromyogram: Literature review and some insights," *Phys. Eng. Sci. Med.*, vol. 43, no. 2, pp. 481–492, Jun. 2020.

[38] M. Bourges, G. R. Naik, and L. Mesin, "Single channel surface electromyogram deconvolution is a useful pre-processing for myoelectric control," *IEEE Trans. Biomed. Eng.*, vol. 69, no. 5, pp. 1767–1775, May 2022.

MATTEO RAGGI received the B.S. and M.S. degrees in biomedical engineering from Politecnico di Torino, in 2019 and 2022, respectively, where he is currently pursuing the Ph.D. degree in electrical, electronics and communications engineering with the Department of Electronics and Telecommunications. His research interests include biomedical signal processing, e-textiles, and wearable devices.
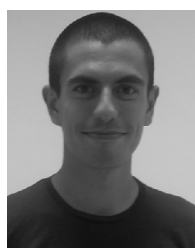
GENNARO BOCCIA received the master's degree in advanced sciences of sport training from the University of Turin, Italy. His Ph.D. was focused on methodological aspects of electromyography (EMG) to study muscle fatigue and muscle coordination. After being a Research Fellow with the University of Verona and a Visiting Researcher with the University of Birmingham, he is currently an Associate Professor of the University of Turin. He is investigating the effects of muscle fatigue on muscle contraction quickness and on physical performances that rely on such a physical capacity. He has adopted the means of high-density surface electromyography to non-invasively monitor the motor units properties and the spatial distribution of electromyographic activity across the muscle.

LUCA MESIN received the Graduate degree in electronics engineering, in 1999, and the Ph.D. degree in applied mathematics from Politecnico di Torino, Italy, in 2003. He is currently an Associate Professor in biomedical engineering and a Supervisor of the Mathematical Biology and Physiology Group, Department of Electronics and Telecommunications, Politecnico di Torino. His current research interests include biomedical image and signal processing, and mathematical modeling.

• • •